Iraqi Journal for Applied Science (IJAS)
Vol. 2, No. 2, June, 2025, pp. 83-89
ISSN: 3006-5828, DOI: 10.69923/5xtj4329

Effect of Increasing Ablation Energy on the Physical Properties of CuO and Al_2O_3 Nanoparticles

Saif Khalel Jasim[1]*, Noor A. Hameed[2], Waleed Hatem Namous[1]
[1]Ministry of Education. Diyala Education Directorate, Diyala, Iraq,
[2]University of Diyala ,Al-Muqdad College of Education, Diyala, Iraq

Article Info

Article history:

Received: 27, 03, 2025
Revised: 24, 05, 2025
Accepted: 03, 06, 2025
Published: 30, 06, 2025

Keywords:

Laser
Ablation
Copper
Aluminum
Nanoparticles

ABSTRACT

In this study, copper (Cu) and aluminium (Al) nanoparticles (NPs) were prepared to study their physical properties in a simple, easy and environmentally friendly way using a switched Nd:YAG laser by bombarding the target placed in a liquid-filled beaker at a rate of 600 pulses per second, an ablation energy of 200 and 400 mJ and a frequency of 2 Hz. The XRD results indicate that cubic symmetry was obtained for copper and also for aluminium. The average nanoparticle size determined by TEM was (20 nm) for copper and the average size of aluminium diameters was (22 nm). As for the optical properties, at 200, and 400 mJ the surface plasmon resonance (SPR) peak for copper was at (295, and 655 nm) while aluminium was at (288, and 289 nm) respectively, and the energy gap for copper was (3.17, and 3.2 eV) and aluminium was (4.6, and 4.7 eV) respectively. These materials are very useful for applications in photocatalysis and sensors.

Corresponding Author:

Saif Khalel Jasim
Ministry of Education. Diyala Education Directorate
Diyala, Iraq
Email: saifalaosy@gmail.com

1. INTRODUCTION

As a new area of study, nanotechnology necessitates accurate methods for describing materials at the nanoscale with the intended prepared materials' physical and chemical characteristics [1]. Only the threshold process of explosive material evaporation from a solid target's surface with the creation of a gas (vapor) plasma cloud through the quick absorption of high-power laser pulse energy in a constrained container would be referred to as "ablation" [2]. First off, laser materials processing has successfully used pulsed laser ablation (PLA) to pierce, label, and precisely remove layers of material in electronics. PLA involves exposing the target to micro and nanosecond pulses followed by femtosecond ones [3,4]. Subsequently, PLA in gas phase and vacuum was effectively employed to atomize targets in mass spectrometry, producing ultrafine powders and thin films [5,6]. The rapid advancement of nanotechnology in the 1990s of the 20th century sparked the use of PLA of bulk objects in liquids to produce nanoparticles (NPs) [7,8]. The dispersions of Ag, Au, Pt, Al, Pd, and Cu nanoparticles in water and organic solvents for the surface enhanced raman scattering (SERS) spectroscopy were achieved in 1993, marking the first intentional application of this approach for the manufacture of nan colloids [9]. Pulsed laser ablation in liquids (PLAL) has grown in popularity and effectiveness over the last 20 years as a method of producing nanoscale materials [10,11]. The absence of a mechanical interaction in the synthesis process and the ability to prepare pure nanoparticles without additional chemicals in the pure solvents straightaway in the form of stable colloids make this method very attractive for biological and medical applications [12,13]. Catalysis, electronics and nonlinear optics are also the areas where the nan colloids synthesized by the PLAL method and nanocrystal line powder obtained via further drying of the dispersions are used [14]. This method is an appropriate tool for obtaining nanomaterials for the study of fundamental properties of substances in the nanostate because of its relatively simple experimental technique and the ability to obtain various types of nanoparticles (from metals to ceramics and polymers) on the same installation [15,16].

The composition, structure, and dimensional properties of the resulting nanoparticles can be further varied by adjusting the laser pulse settings and using different solvents with precursor additives [17]. There are currently thousands of published original research studies, reviews, and monographs covering different facets of the PLAL for nanostructure creation [18,19]. They also take into account typical methods for obtaining PLAL and characterizing particular nanomaterials. Nonetheless, there is still a strong interest in this type of research [20]. One explanation for this is the need for nanomaterials with certain functional characteristics for a range of uses [21, 22]. However, there are three primary objectives that remain unfulfilled: efficient regulation of the nanoparticles' dimensional properties and structure [4].

2. METHOD

2.1 PREPARATION NANOPARTICLES BY PLAL

Pulsed laser ablation experiments were performed using a pulsed Nd:YAG laser with an output energy of 200, and 400 mJ at a wavelength of 1064 nm, and the liquid medium was distilled water with 99% purity. The pulse width and repetition rate of this laser were 10 ns, 2 Hz, and pulses number 600 pulse/sec. A vertical PLAL configuration (8 cm focal length) was used to direct and focus the laser beam on the Cu, and Al metal target. The target was a metal plate with dimensions (1*1*0.2 mm) of 99.9% purity, immersed in distilled water, which was used as the incubation medium for the nanomaterials to improve the ablation and was performed under standard conditions. A target placed in a 5 mL baker filled with distilled water is bombarded with a number of pulses, creating a plasma plume and a cloud bubble when a pulse hits the metal target surface [23], as shows in figure (1).

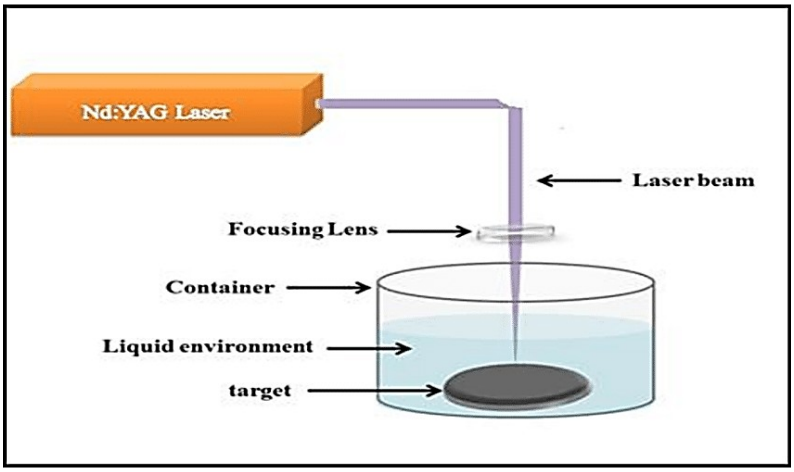

Figure 1: Schematic of an electrochemical etching setup.

2.2 CHARACTERIZATION

he physical properties of nanoparticles are diagnosed and characterized through X-ray measurements, which can characterize the nanostructure, crystalline phases, miller coefficients and granular size calculation, as well as using transmission electron microscopy, through which the size of the nanoparticles can be known by depositing the liquid on the salads in the form of drops casting using the distillation method, the absorbance of the material is known by measuring the UV-visible spectrometer to determine the surface plasmon resonance site at any wavelength for CuO and aluminum, and through the absorbance, calculate the energy gap for copper and aluminum oxides. The data was analyzed by the software program (image j) to calculate the size of the nanoparticles, while the statistical plot of the average size of the nanoparticle diameters, the absorbance plot and the energy gap by (origin lab 2018).

3. RESULTS AND DISCUSSION

3.1 XRD ANALYSIs:

Figure (2) shows the X-ray diffraction results for of copper oxide nanoparticles prepared at ablation energy (400 mJ), with results corresponding to the international label (JCPDSNo.04-0836). with cubic symmetry obtained two peaks at angles (44.27, 52.34) that correspond to levels (200) and (111), respectively, showing two peaks at angles (44.21, 52.25) that correspond to the levels (200) and (111) respectively, and a prominent peak at (66.45) that corresponds to (220).

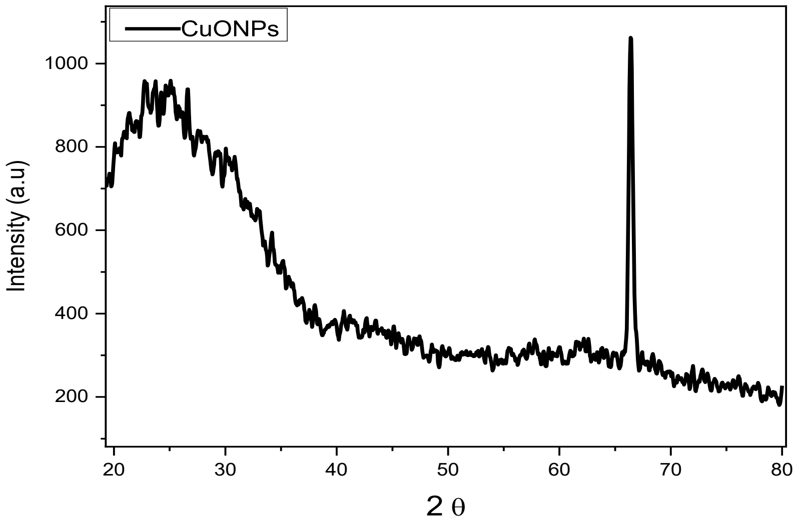

Figure.2 XRD diffraction results CuONPs.

While figure (3) shows the Xrd diffraction results of the prepared aluminum oxide nanoparticles (Al_2O_3NPs) at ablation energy (400 mJ), the results obtained indicate that the peaks obtained for the aluminum nanoparticles are very similar to the researcher (Chang, Yu-Ling, et al)[24]. The intensities seem to vary but the crystal planes are similar, with prominent peaks appearing at (38, 44, 65, and 78) degrees which correspond to the (111), (200), (220), and (311) planes, respectively, corresponding to the international label (ICSD 53773).

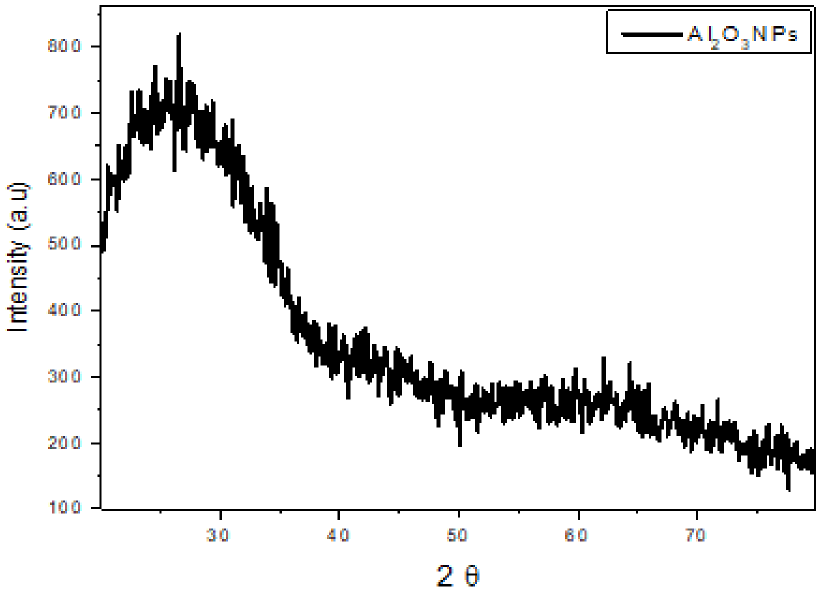

Figure 3: XRD diffraction results Al2O3NPs.

3.2 TEM ANALYSIS

Figure 4 (a) shows the transmission electron microscopy (TEM) results for a sample of copper nanoparticles (CuONPs) prepared in distilled water medium at 200 mJ. The TEM measurement shows that semispherical and spherical shapes are obtained, with a size range of (3 – 51 nm) and average particle diameters of (22 nm), as shows figure 4 (c) while the sample the prepared at 400 mJ, were spherical shapes obtained, size range (2 – 46 nm) and average particle diameters (20 nm), figure 4 (b, and d). Figure 5 (a, and c) shows a sample of (Al_2O_3NPs) prepared in distilled water medium at 200 mJ, the TEM measurement showed that spherical particles were obtained, ranging in size from (2-45 nm) with an average particle diameter of (15 nm). while the sample the prepared at 400 mJ spherical shapes were obtained, with a size range (2–38 nm) and average particle diameters (14 nm) figure 5 (b, and d). By increasing the energy from 200 to 400 mJ, a greater concentration of nanoparticles, more numerous and smaller in size, was obtained.

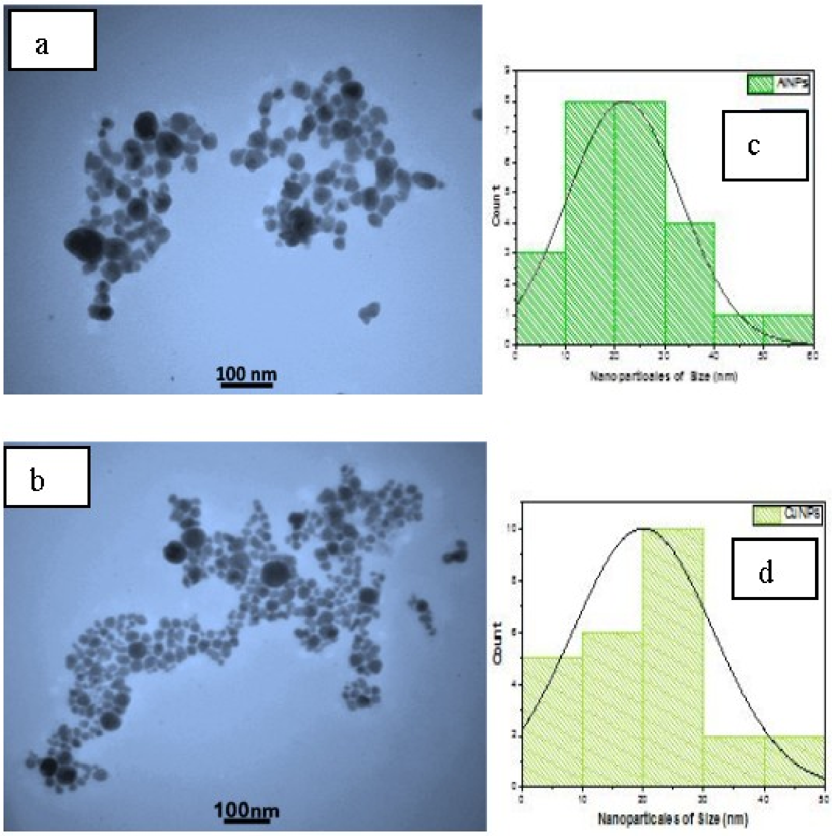

Figure 4: Results CuONPs a- TEM image at 200 mJ, b- TEM image at 400 mJ, c- Histogram at200 mJ , and d- Hostgram 400 mJ

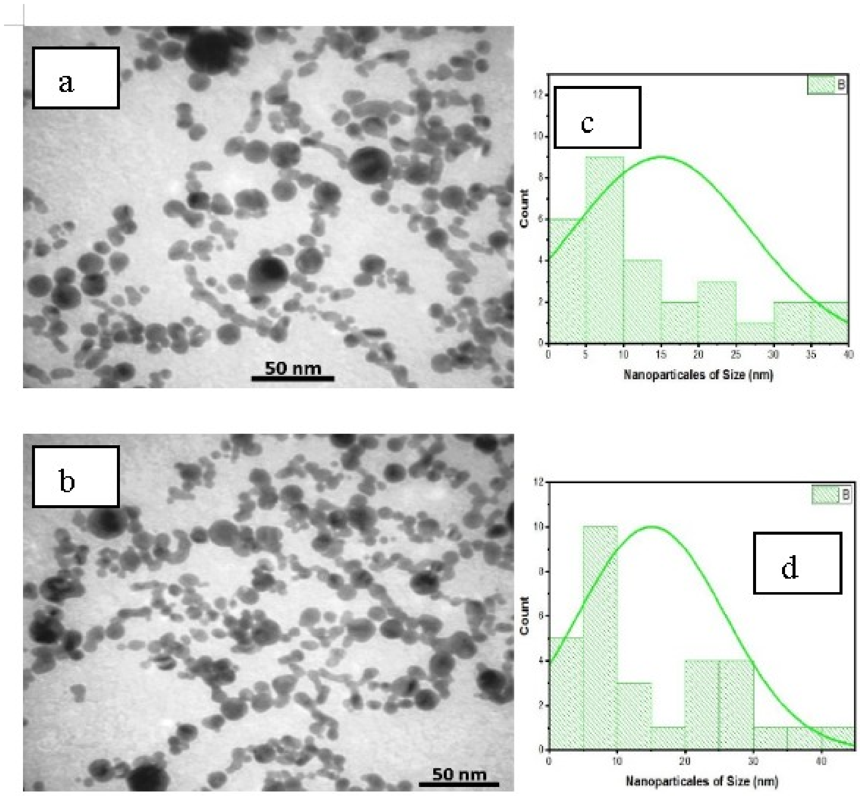

Figure 5: Results Al2O3NPs, a- TEM image at 200 mJ, b- TEM image at 400 mJ, c- Histogram at200 mJ , and d- Histogram 400 mJ

Table 1 Result TEM for CuONP, and Al2O3NP

Energy ablation	CuONP		Al_2O_3NP	
	Average size (nm)	Ship NPs	Average size (nm)	Ship NPs
200 mJ	22 nm	semispherical and spherical	14 nm	spherical
400 mJ	20 nm	spherical	15 nm	spherical

3.3 OPTICAL ANALYSIS
3.3.1 UV-VIS SPECTRA

Figure (5 and 6) shows the UV-VIS measurement results of Cu nanoparticles and Al nanoparticles prepared at 200 and 400 mJ, showing the color change from colourless to greenish brown for CuO nanoparticles (Insert 1), while Al_2O_3 nanoparticles from colorless to white (Insert 2), this color change was gradual and the color stability of the nanoparticles was very high even after more than five months of preparation. The surface 0.65 a.u.) respectively, while the SPR peak of Al2O3 nanoparticles was obtained at the wavelength (288 nm), with absorbance (0.6, and 1.75 a.u.).

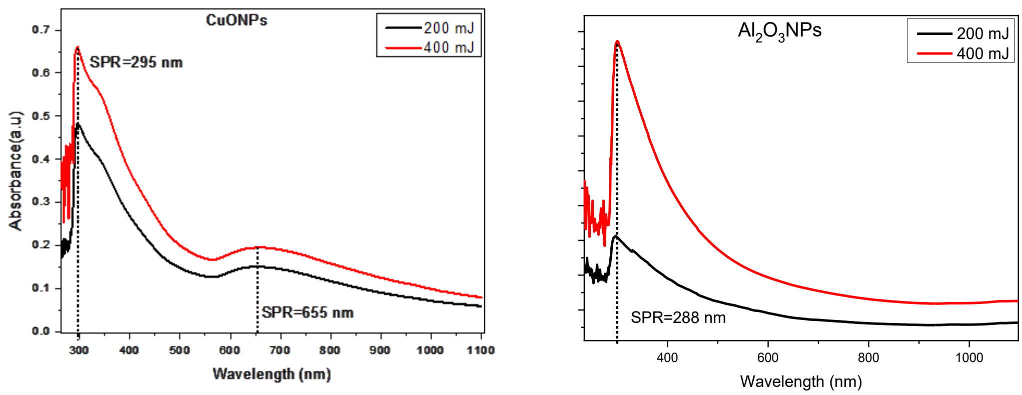

Figure 6: UV-VIS measurement results a- CuONPs, b- Al2O3NPs

3.3.2 ENERGY GAP

Figure (5) shows the energy gap for copper nanoparticles and aluminum nanoparticles, where the energy gap is calculated by Tau's law according to equation (1)

$$\propto hv=A(hv-E\_g)^\wedge(1/2) \qquad (1)$$

Where (∝) is the absorption coefficient and (hv) is the photon energy and by drawing between (hv) on the x-axis and (∝ hv) on the y-axis, then the energy gap can be determined at (hv=0)[25] and as in figure 5. (a, and b), the energy gap was (3.17, and 3.2 eV) for CuONPs. while the energy gap value for Al2O3NPs n was (4.6, and 4.7 eV) figure 5. (c, and d).

Table 2 Result Optical properties for CuONP, and Al2O3NP

Result		CuONPs	Al_2O_3NPs
SPR(nm)	200 mJ	297-655	**288**
Abs.(a.u)		0.15- 0.48	0.6
Eg.(eV)		3.17	4.6
SPR(nm)	400 mJ	295-655	**288**
Abs.(a.u)		0.19- 0.65	1. 75
Eg.(eV)		3.2	4.7

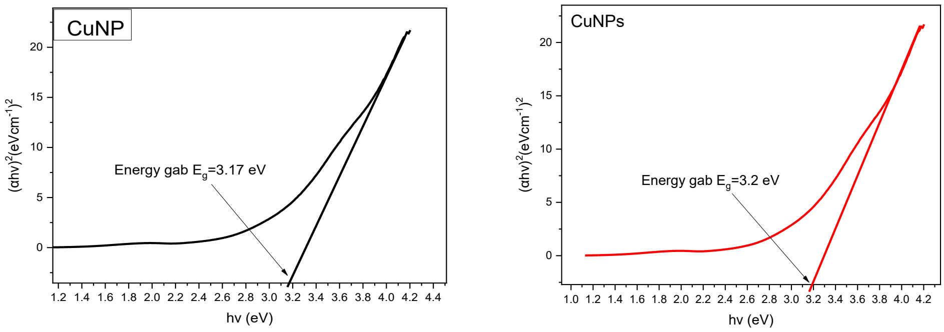

Figure 7: Energy gap measurement for CuONPs a-, at 200 mJ, b- at 400 mJ.

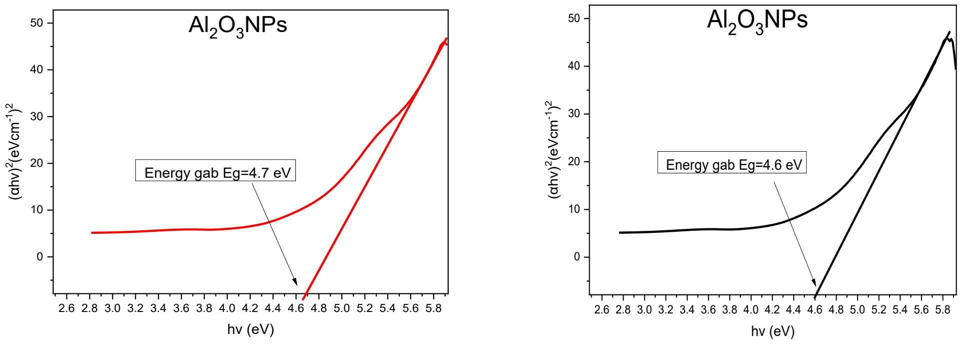

Figure 8: Energy gap measurement for Al2O3NPs a-at 200 mJ, b- at 400 mJ.

4. CONCLUSION

The physical properties of copper and aluminum nanoparticles were studied by pulsed laser ablation, where using laser parameters at 200 and 400 mJ energy and 600 pulses per second in water distilled media, the nanosize was controlled to obtain an average size of less than 50 nm, the surface plasmon resonance of CuONPs was determined at 295, and 655 nm, while Al_2O_3NPs was at 288 nm. and calculate the energy gap through absorbance, where an energy gap of 3.2, and 3.17 eV receptivity was obtained for copper oxide nanoparticles, while the energy gap was 4.6, and 4.7 eV receptivity, for aluminum oxide nanoparticles.

Acknowledgment

The authors would like to thank the University of Tikrit/College of Science/Department of Physics for the technical support to complete this work in their laboratories.

REFERENCES

[1] M. Stafe, A. Marcu, and N. N. Puscas, Pulsed Laser Ablation of Solids. Berlin: Springer, 2014.
[2] M. Dell'Aglio et al., "Mechanisms and processes of pulsed laser ablation in liquids during nanoparticle production," Applied Surface Science, vol. 348, pp. 4–9, 2015.
[3] E. Fazio et al., "Nanoparticles engineering by pulsed laser ablation in liquids: Concepts and applications," Nanomaterials, vol. 10, no. 11, p. 2317, 2020.
[4] S. K. Jasim, A. M. Shano, and S. K. Adnan, "Zinc Oxide Poly Crystals Heterojunction and Infrared-Blind UV-Photodetector," unpublished, 2024.
[5] M. Darroudi et al., "Preparation and characterization of gelatin mediated silver nanoparticles by laser ablation," Journal of Alloys and Compounds, vol. 509, no. 4, pp. 1301–1304, 2011.
[6] E. A. Mwafy and A. M. Mostafa, "Efficient removal of Cu (II) by SnO_2/MWCNTs nanocomposite by pulsed laser ablation method," Nano-Structures & Nano-Objects, vol. 24, p. 100591, 2020.
[7] W. Zhao et al., "Percussion drilling hole in Cu, Al, Ti and Ni alloys using ultra-short pulsed laser ablation," Materials, vol. 13, no. 1, p. 31, 2019.
[8] P. K. Baruah, A. K. Sharma, and A. Khare, "Role of confining liquids on the properties of Cu@Cu_2O nanoparticles synthesized by pulsed laser ablation and a correlative ablation study of the target surface," RSC Advances, vol. 9, no. 26, pp. 15124–15139, 2019.
[9] A. S. Jasim, S. K. Jasim, and A. A. Habeeb, "Synthesis of Cinnamon Nanoparticles by Using Laser Ablation Technique," Iraqi Journal of Physics, vol. 19, no. 49, pp. 7–14, 2021.

[10] A. H. Ahmed, A. S. Jasim, and S. K. Jasim, "Synthesis of Gold Nanoparticles by Pulsed Laser Ablation and its Study Physical and Mechanical Properties," International Journal of Nanoelectronics and Materials, vol. 17, no. 4, pp. 634–641, 2024.
[11] N. O. E. Zamora-Romero et al., "Synthesis of molybdenum oxide nanoparticles by nanosecond laser ablation," Materials Chemistry and Physics, vol. 240, p. 122163, 2020.
[12] S. K. Jasim, A. S. Jasim, and A. A. Habeeb, "Growth Cinnamon Nanoparticles in Different Liquid by Pulsed Laser Ablation in Liquid PLAL," Mesopotamian Journal of Pure Science (MJPS), vol. 8, no. 2, 2021.
[13] R. M. Altuwirqi et al., "Synthesis and characterization of aluminum nanoparticles prepared in vinegar using a pulsed laser ablation technique," Journal of Nanomaterials, vol. 2020, no. 1, p. 1327868, 2020.
[14] P. Sutradhar, N. Debnath, and M. Saha, "Microwave-assisted rapid synthesis of alumina nanoparticles using tea, coffee and triphala extracts," Advances in Manufacturing, vol. 1, pp. 357–361, 2013.
[15] A. H. Ahmed, A. S. Jasim, and S. K. Jasim, "Silver Oxid Nanoparticles Prepared by Pulsed Laser Ablation in Liquid and Thier Study Physical Properties," Web of Semantics: Journal of Interdisciplinary Science, vol. 2, no. 2, pp. 1–9, 2024.
[16] Q. Zhang et al., "One-Step Laser Preparation of Unidirectional Liquid Spontaneous Transport Structures," Surface Topography: Metrology and Properties, 2024.
[17] M. A. Gondal et al., "Phase transformation and structural characterization studies of aluminum oxide (Al_2O_3) nanoparticles synthesized using an elegant pulsed laser ablation in liquids technique," Nanoscience and Nanotechnology Letters, vol. 8, no. 11, pp. 953–960, 2016.
[18] S. K. Jasim et al., "Determine surface plasmon resonance and effect parameters laser ablation on Cu and Zn nanoparticles," AIP Conference Proceedings, vol. 3219, no. 1, AIP Publishing, 2024.
[19] A. Nyabadza, M. Vazquez, and D. Brabazon, "A review of bimetallic and monometallic nanoparticle synthesis via laser ablation in liquid," Crystals, vol. 13, no. 2, p. 253, 2023.
[20] A. R. Sadrolhosseini et al., "Laser ablation technique for synthesis of metal nanoparticle in liquid," in Laser Technology and its Applications, pp. 63–83, 2019.
[21] A. Subhan, A.-H. I. Mourad, and Y. Al-Douri, "Influence of laser process parameters, liquid medium, and external field on the synthesis of colloidal metal nanoparticles using pulsed laser ablation in liquid: A review," Nanomaterials, vol. 12, no. 13, p. 2144, 2022.
[22] J. M. Hussein et al., "Study and characterization ZnO nanoparticles prepared by switched laser Nd:YAG," Indonesian Journal of Material Research, vol. 2, no. 3, pp. 73–78, 2024.
[23] T. Y. Sabri et al., "Preparation and Study Ag Nanoparticles via PLAL Technique: Influence of Different Number of Pulses," International Journal of Nanoelectronics and Materials, vol. 17, no. 1, pp. 45–51, 2024.
[24] Y.-L. Chang et al., "Aluminum plasmonic nanoclusters for paper-based surface-enhanced Raman spectroscopy," Analytical Chemistry, vol. 94, no. 47, pp. 16319–16327, 2022.
[25] J. Zhang et al., "Colloidal metal nanoparticles prepared by laser ablation and their applications," ChemPhysChem, vol. 18, no. 9, pp. 986–1006, 2017.